Distribution System Restructuring: Distribution LMP Via Unbalanced ACOPF

Yikui Liu, *Student Member, IEEE,* Jie Li, *Member, IEEE,* Lei Wu, *Senior Member, IEEE*

***Abstract*—The emerging distribution system with a proliferation of distributed energy resources (DER) and flexible demand assets is expected to experience the restructuring process, just as what has been happening in the transmission system. This paper introduces the distribution locational marginal price (DLMP) as an effectively economic signal to quantify marginal cost for supplying next incremental loads at different phases of individual nodes. DLMP is calculated by solving the unbalanced AC optimal power flow (ACOPF) problem of distribution systems, with the objective of minimizing system operation cost. Indeed, in order to derive effective DLMPs, global optimal solution to the non-convex unbalanced ACOPF problem with a zero duality gap needs to be obtained. This paper solves the unbalanced ACOPF problem via the moment relaxation based semidefinite programming (SDP) model. System sparsity is explored to accelerate the computational performance. In addition, a hierarchical approach is proposed to recover a good enough feasible solution to the original ACOPF, when the sparse moment relaxation based SDP model is inexact. Numerical case studies on a modified IEEE 34-bus system evaluate the effectiveness and validity of the proposed approach. DLMP based revenue adequacy of the distribution system is also analyzed.**

***Index Terms*—Distribution LMP, distribution system restructuring, revenue adequacy.**

NOMENCLATURE

Sets and Indices:

$\mathbb{C},\mathbb{N},\mathbb{R}$	Set of complex/natural/real numbers
e_n^{ϕ}	Standard basis vector of $\mathbb{R}^{3N}$ with the $(3n+\phi)^{\text{th}}$ element being "1", where ϕ =1, 2, and 3 represent phases *a*, *b*, and *c*, respectively
k	Index of voltage variable subsets
m, n	Indices of buses, ranging from 0 to (*N*-1)
N	Total number of buses
$\mathbf{\Omega}$	Set of buses
$\mathbf{\Omega}_f$	Set of buses where flexible loads (FL) are connected to
$\mathbf{\Omega}_g$	Set of DER buses and the distribution substation bus
$\mathbf{\Omega}_n$	Set of buses adjacent to bus *n*
$\mathbf{\Psi}$	Set of phases, i.e., $\mathbf{\Psi}=\{a,b,c\}$
ϕ,ρ	Indices of phases

Variables:

$P_{Gn}^{\phi},Q_{Gn}^{\phi}$	Real/reactive power injection from the DER at phase ϕ of bus *n*
$P_{Dn}^{\phi},Q_{Dn}^{\phi}$	Real/reactive power load at phase ϕ of bus *n*
$\mathbf{V}$	$\mathbf{V}=\left[Re(\dot{\mathbf{V}})^T \;\; Im(\dot{\mathbf{V}})^T\right]^T$, where $\dot{\mathbf{V}}=[V_0^a\ V_0^b\ V_0^c\ \ldots\ V_{N-1}^a\ V_{N-1}^b\ V_{N-1}^c]^T$, $V_n^{\phi}=V_n^{re,\phi}+j\cdot V_n^{im,\phi}$ is complex voltage at phase ϕ of bus *n*
$\hat{\mathbf{V}}$	Augmented vector of $[1\quad \mathbf{V}^T]^T$

Constants:

$P_{Gn}^{\phi\,min},P_{Gn}^{\phi\,max}$	Real power lower/upper bound of the DER at phase ϕ of bus *n*
$Q_{Gn}^{\phi\,min},Q_{Gn}^{\phi\,max}$	Reactive power lower/upper bound of the DER at phase ϕ of bus *n*
$P_{Dn}^{\phi\,min},P_{Dn}^{\phi\,max}$	Real power lower/upper bound of the FL at phase ϕ of bus *n*
$Q_{Dn}^{\phi\,min},Q_{Dn}^{\phi\,max}$	Reactive power lower/upper bound of the FL at phase ϕ of bus *n*
$\lvert V_n^{\phi}\rvert^{min}$	Voltage lower bound at phase ϕ of bus *n*
$\lvert V_n^{\phi}\rvert^{max}$	Voltage upper bound at phase ϕ of bus *n*
$\tilde{\mathbf{V}}_0$	Given voltage values at the distribution substation bus, i.e. $\tilde{\mathbf{V}}_0=[V_0^{re,a}\ V_0^{re,b}\ V_0^{re,c}\ V_0^{im,a}\ V_0^{im,b}\ V_0^{im,c}]^T$
ε	Prespecified convergence threshold

Symbols:

$card(\cdot)$	Number of elements in a vector or a set
$Im(\cdot),Re(\cdot)$	Imaginary/real part
$size(\cdot)$	Dimension of a matrix
$tr(\cdot)$, $(\cdot)^T$, $\lvert\cdot\rvert$	Trace/ transpose/ magnitude
$\mathbf{0}$	Matrix with all zeros
$\tilde{\cdot}$	Given solution to a variable
$\hat{\cdot}$	An augmented variable vector or a parameter matrix

I. INTRODUCTION

The electricity distribution sector is envisioned to include a deeper penetration of distributed energy resources (DERs), plug-in electrical vehicles, plug-and-play energy storage devices, and demand response assets. In order to effectively integrate these new technologies, modern distribution systems are expected to experience a restructuring process, just as what has been happening in transmission systems [1].

Distribution locational marginal price (DLMP), which reflects marginal cost of supplying next incremental loads in different locations, has been studied to provide electricity consumers and DER owners/investors effective economic signals for optimizing the size and location of their assets [2]-[4]. DLMP is introduced to the distribution system for the first time by [5] with the purpose of properly allocating system losses. Since in a low voltage distribution network resistances

This work was supported in part by the U.S. National Science Foundation grant PFI:BIC-1534035. Y. Liu, J. Li, and L. Wu are with Electrical and Computer Engineering Department, Clarkson University, Potsdam, NY 13699 USA. (E-mail: yikliu@clarkson.edu, jieli@clarkson.edu, lwu@clarkson.edu).

of distribution lines are relatively large comparing to transmission lines, system losses constitute a significant portion of energy to be delivered. DLMPs are able to reflect the increase in system operation cost due to increased losses when supplying the next incremental load at a certain bus. Therefore, system loss is one of the main factors that influence values of DLMPs.

In a distribution network, bus voltage regulation is a critical issue commonly faced by distribution system operators. Specifically, with a proliferation of DERs and flexible loads (FLs), voltage violations, either constraining the lower bound (due to large demands of FLs) or the upper bound (due to large power injections of DERs), become more noticeable. Thus, in order to satisfy bus voltage limitations, DERs and FLs are always not dispatched economically. That is, expensive DERs may be dispatched and highly beneficial FLs may be curtailed to alleviate violations on voltage lower bounds. Similarly, cheap DERs may be shut down and low beneficial FLs may be awarded to mitigate violations on voltage upper bounds. Remarkably, as an economic signal, DLMPs could also properly reflect the impact of voltage limitations on economical operation of the distribution system.

Distribution systems present unique characteristics comparing to transmission systems. Essentially, distribution systems are unbalanced because of unbalanced loads, unbalanced DERs, and unbalanced/untransposed line segments. In addition, phase missing configuration is also common in practice. In turn, the three phases are generally operated in different conditions. Thus, unique DLMPs for all three phases, which are exclusively utilized in balanced systems, are unable to accurately reflect operation conditions of unbalanced systems and provide effective economic signals for all three phases. In this paper, DLMPs are assigned to different phases of different buses in the distribution system. That is, at a same bus, DLMPs of different phases may be different. The phase based economic signals provided by DLMPs can effectively incentivize consumers and DER owners/investors to optimally adjust their connection topologies (i.e., which bus and which phase), which would ultimately drive the distribution system to be operated in a more balanced manner.

This paper focuses on the unbalanced three-phase radial distribution system, which includes four-conductor multi-grounded or three-conductor single-grounded lines, wye-wye grounded transformers, and wye grounded loads. DLMPs are defined and constructed via Lagrangian multipliers of corresponding constraints in AC optimal power flow (ACOPF) problem with the objective of minimizing total operation cost of the distribution system. In order to derive exact price signals via the ACOPF problem, the following two conditions should be met: (i) the global optimal primal and dual solutions of ACOPF can be obtained; and (ii) the strong duality between the primal and its dual problem can be guaranteed. Zero duality gap at the global optimal solution will ensure that optimal Lagrangian multipliers can accurately reflect deviations of the objective value with respect to changes in bounds of corresponding constraints.

Indeed, ACOPF problem is nonconvex because of the nonlinear relationship between voltages and net complex power injections at individual buses [6]. In turn, the above two conditions may not be satisfied in general. Recently, convex relaxation techniques have been applied to obtain global optimal solution and eliminate the dual gap. A rank relaxation based semidefinite programming (SDP) model for ACOPF of single-phase systems was discussed in [7], which is convex and holds the strong duality condition. However, as rank relaxation based SDP model enlarges feasible region of the origin ACOPF, optimal solution to the rank relaxation based SDP model may be infeasible to the origin ACOPF [8]-[10], i.e., the rank relaxation could be inexact. Some works explored conditions under which the rank relaxation based SDP model is exact [11]-[13]. Remarkably, [14] introduced graph transformed from the structure of the ACOPF problem for analyzing exactness of the rank relaxation. [15]-[16] provided a comprehensive overview on sufficient conditions for various relaxation models and approaches. However, all of them are restricted to single-phase radial or weakly meshed systems, in which graphs of corresponding ACOPF problems are also radial or weakly meshed.

Indeed, although unbalanced three-phase distribution systems are usually radial, graphs transformed from the structure of ACOPF problems are strongly meshed. For ACOPF problems with meshed graphs, sufficient conditions on exactness of the rank relaxation based SDP approach cannot be satisfied in practice [14]. In turn, alternative tighter convex relaxation techniques have been explored. Inspired by the seminal work of Lasserre [17], ACOPF was formulated as a polynomial optimization problem and solved by a hierarchy of moment relaxation based SDP models [18]. High order moment relaxation is tighter than rank relaxation [19], and exactness may be achieved for more general systems. As computation burden could easily become intractable when a high order moment relaxation is adopted, [19] further exploited sparsity of networks and proposed a sparse moment relaxation technique [20] for improving the computational performance.

In this paper, the ACOPF problem for unbalanced three-phase distribution system is formulated as a sparse moment relaxation based SDP model [21] to enhance the computational efficiency. In addition, to deal with possible inexactness of the sparse moment relaxation based SDP model, a two-stage hierarchical approach is proposed to obtain the global optimal solution or recover a good enough feasible solution to the original ACOPF. Lagrangian multipliers of certain constraints in the ACOPF problem are utilized to construct DLMPs. Sensitivity of DLMPs at DER buses and the revenue adequacy are analyzed.

The main contributions of the paper include:

1) DLMPs for unbalanced three-phase radial distribution systems are defined and constructed via corresponding Lagrangian multipliers of the ACOPF problem, which is formulated as a moment relaxation based SDP model.

2) The running intersection property of the ACOPF problem

for unbalanced three-phase distribution systems is analyzed to derive the sparse moment relaxation based SDP model, which would significantly improve the computational efficiency.

3) A two-stage hierarchical approach is proposed to obtain the global optimal solution or recover a good enough feasible solution to the original ACOPF problem.

The rest of the paper is organized as follows. Moment relaxation and sparse moment relaxation based SDP models for ACOPF of unbalanced three-phase distribution systems are formulated in Section II. In section III, DLMPs are defined and discussed. Numerical case studies are presented in Section IV. The conclusions are drawn in Section V.

II. Moment Relaxation Based Unbalanced ACOPF

A. ACOPF for Unbalanced Three-Phase Distribution Systems

For four-conductor multi-grounded neutral and three-conductor single-grounded neutral distribution systems, the line impedance matrix can be written as a 3×3 phase frame matrix. Similarly, the impedance matrix of three-phase wye-wye solidly grounded transformers is also a 3×3 phase frame matrix. Thus, for an *N*-node distribution system (including the distribution substation bus indexed as 0), the three-phase nodal admittance matrix $\mathbf{Y} \in \mathbb{C}^{3N\times 3N}$ can be constructed by combining the distribution network topology and 3×3 phase frame matrices of individual assets.

Net real and reactive power injections in phase ϕ of bus n from all connected distribution lines are calculated via $\widehat{\mathbf{V}} \cdot \widehat{\mathbf{\Phi}}_{P,n}^{\phi} \cdot \widehat{\mathbf{V}}^T$ and $\widehat{\mathbf{V}} \cdot \widehat{\mathbf{\Phi}}_{Q,n}^{\phi} \cdot \widehat{\mathbf{V}}^T$, where $\widehat{\mathbf{\Phi}}_{P,n}^{\phi}$ and $\widehat{\mathbf{\Phi}}_{Q,n}^{\phi}$ are given in (1)-(4).

$$\mathbf{Y}_n^{\phi} \triangleq \mathbf{e}_n^{\phi} \cdot \left(\mathbf{e}_n^{\phi}\right)^T \cdot \mathbf{Y} \tag{1}$$

$$\mathbf{\Phi}_{P,n}^{\phi} \triangleq \frac{1}{2}\begin{bmatrix} Re\left(\mathbf{Y}_n^{\phi} + \left(\mathbf{Y}_n^{\phi}\right)^T\right) & Im\left(\left(\mathbf{Y}_n^{\phi}\right)^T - \mathbf{Y}_n^{\phi}\right) \\ Im\left(\mathbf{Y}_n^{\phi} - \left(\mathbf{Y}_n^{\phi}\right)^T\right) & Re\left(\mathbf{Y}_n^{\phi} + \left(\mathbf{Y}_n^{\phi}\right)^T\right) \end{bmatrix} \tag{2}$$

$$\mathbf{\Phi}_{Q,n}^{\phi} \triangleq \frac{1}{2}\begin{bmatrix} Im\left(\mathbf{Y}_n^{\phi} + \left(\mathbf{Y}_n^{\phi}\right)^T\right) & Re\left(\mathbf{Y}_n^{\phi} - \left(\mathbf{Y}_n^{\phi}\right)^T\right) \\ Re\left(\left(\mathbf{Y}_n^{\phi}\right)^T - \mathbf{Y}_n^{\phi}\right) & Im\left(\mathbf{Y}_n^{\phi} + \left(\mathbf{Y}_n^{\phi}\right)^T\right) \end{bmatrix} \tag{3}$$

$$\widehat{\mathbf{\Phi}}_{P,n}^{\phi} \triangleq \begin{bmatrix} 0 & \mathbf{0} \\ \mathbf{0} & \mathbf{\Phi}_{P,n}^{\phi} \end{bmatrix} \quad \widehat{\mathbf{\Phi}}_{Q,n}^{\phi} \triangleq \begin{bmatrix} 0 & \mathbf{0} \\ \mathbf{0} & \mathbf{\Phi}_{Q,n}^{\phi} \end{bmatrix} \tag{4}$$

Operation costs of DERs and benefit functions of FLs in phase ϕ of bus n are represented by (5) and (6), respectively.

$$C_n^{\phi}\left(P_{Gn}^{\phi}\right) = c_{n,2}^{\phi} \cdot \left(P_{Gn}^{\phi}\right)^2 + c_{n,1}^{\phi} \cdot P_{Gn}^{\phi} + c_{n,0}^{\phi}, \quad \forall n \in \mathbf{\Omega}_g \tag{5}$$

$$B_n^{\phi}\left(P_{Dn}^{\phi}\right) = b_{n,2}^{\phi} \cdot \left(P_{Dn}^{\phi}\right)^2 + b_{n,1}^{\phi} \cdot P_{Dn}^{\phi} + b_{n,0}^{\phi}, \quad \forall n \in \mathbf{\Omega}_f \tag{6}$$

Given electricity price c_0 of all three phases at the distribution substation bus, the unbalanced three-phase distribution ACOPF problem is formulated as a polynomial programming model (7). The objective (7a) minimizes the distribution system operation cost. (7b)-(7e) are real and reactive power balance in each phase of each bus. (7f)-(7i) are real and reactive power capacity limits of DERs and FLs. (7j) is bus voltage magnitude limit, where $\widehat{\mathbf{\Phi}}_{V,n}^{\phi}$ is defined in (7k). (7l) sets reference voltages for the distribution substation bus.

$$min_{\widehat{\mathbf{V}}, P_{Dn}^{\phi}, Q_{Dn}^{\phi}, P_{Gn}^{\phi}, Q_{Gn}^{\phi}} \begin{Bmatrix} \sum_{\phi\in\mathbf{\Psi}} c_0 \cdot P_{G0}^{\phi} + \sum_{n\in\mathbf{\Omega}_g} \sum_{\phi\in\mathbf{\Psi}} C_n^{\phi}\left(P_{Gn}^{\phi}\right) \\ - \sum_{n\in\mathbf{\Omega}_f} \sum_{\phi\in\mathbf{\Psi}} B_n^{\phi}\left(P_{Dn}^{\phi}\right) \end{Bmatrix} \tag{7a}$$

$$\widehat{\mathbf{V}}^T \cdot \widehat{\mathbf{\Phi}}_{P,n}^{\phi} \cdot \widehat{\mathbf{V}} = P_{Gn}^{\phi} - P_n^{\phi\, fix}, \quad \forall n \notin \mathbf{\Omega}_g \tag{7b}$$

$$\widehat{\mathbf{V}}^T \cdot \widehat{\mathbf{\Phi}}_{Q,n}^{\phi} \cdot \widehat{\mathbf{V}} = Q_{Gn}^{\phi} - Q_n^{\phi\, fix}, \quad \forall n \notin \mathbf{\Omega}_g \tag{7c}$$

$$\widehat{\mathbf{V}}^T \cdot \widehat{\mathbf{\Phi}}_{P,n}^{\phi} \cdot \widehat{\mathbf{V}} = -P_{Dn}^{\phi}, \quad \forall n \in \mathbf{\Omega}_f \tag{7d}$$

$$\widehat{\mathbf{V}}^T \cdot \widehat{\mathbf{\Phi}}_{Q,n}^{\phi} \cdot \widehat{\mathbf{V}} = -Q_{Dn}^{\phi}, \quad \forall n \in \mathbf{\Omega}_f \tag{7e}$$

$$P_{Gn}^{\phi\, min} \le P_{Gn}^{\phi} \le P_{Gn}^{\phi\, max}, \quad \forall n \in \mathbf{\Omega}_g \tag{7f}$$

$$Q_{Gn}^{\phi\, min} \le Q_{Gn}^{\phi} \le Q_{Gn}^{\phi\, max}, \quad \forall n \in \mathbf{\Omega}_g \tag{7g}$$

$$P_{Dn}^{\phi\, min} \le P_{Dn}^{\phi} \le P_{Dn}^{\phi\, max}, \quad \forall n \in \mathbf{\Omega}_f \tag{7h}$$

$$Q_{Dn}^{\phi\, min} \le Q_{Dn}^{\phi} \le Q_{Dn}^{\phi\, max}, \quad \forall n \in \mathbf{\Omega}_f \tag{7i}$$

$$\left(\left|V_n^{\phi}\right|^{min}\right)^2 \le \widehat{\mathbf{V}}^T \cdot \widehat{\mathbf{\Phi}}_{V,n}^{\phi} \cdot \widehat{\mathbf{V}} \le \left(\left|V_n^{\phi}\right|^{max}\right)^2 \tag{7j}$$

$$\widehat{\mathbf{\Phi}}_{V,n}^{\phi} \triangleq \begin{bmatrix} 0 & \mathbf{0} \\ \mathbf{0} & \mathbf{\Phi}_{V,n}^{\phi} \end{bmatrix}, \text{where } \mathbf{\Phi}_{V,n}^{\phi} \triangleq \begin{bmatrix} \mathbf{e}_n^{\phi}\left(\mathbf{e}_n^{\phi}\right)^T & \mathbf{0} \\ \mathbf{0} & \mathbf{e}_n^{\phi}\left(\mathbf{e}_n^{\phi}\right)^T \end{bmatrix} \tag{7k}$$

$$\left[V_0^{re,a} \;\; V_0^{re,b} \;\; V_0^{re,c} \;\; V_0^{im,a} \;\; V_0^{im,b} \;\; V_0^{im,c}\right]^T = \widetilde{\mathbf{V}}_0 \tag{7l}$$

B. Moment Relaxation Approach

The following definitions are presented first. A monomial M_o consisting of elements in $\widehat{\mathbf{V}}$ is defined as $M_o^{\mathbf{\Gamma}}(\widehat{\mathbf{V}}) = \prod_{\eta_n^{re,\phi}, \eta_n^{im,\phi} \in \mathbf{\Gamma}} \left[\left(V_n^{re,\phi}\right)^{\eta_n^{re,\phi}} \cdot \left(V_n^{im,\phi}\right)^{\eta_n^{im,\phi}}\right]$, where $\eta_n^{re,\phi}$ and $\eta_n^{im,\phi} \in \mathbb{N}$. A polynomial P_o including elements in $\widehat{\mathbf{V}}$ is defined as $P_o(\widehat{\mathbf{V}}) = \sum_{\mathbf{\Gamma}_j\in\mathbf{P}} \left[c_j \cdot M_o^{\mathbf{\Gamma}_j}(\widehat{\mathbf{V}})\right]$, where $\mathbf{P} = \{\mathbf{\Gamma}_1, \mathbf{\Gamma}_2, \ldots, \mathbf{\Gamma}_J | J \in \mathbb{N}\}$. The Riesz linear function is defined as in (8), and can be extended to the polynomial matrix form as in (9). $\widehat{\mathbf{V}}$ is augmented to $\widehat{\mathbf{V}}_{\gamma}$ as shown in (10). Specifically, when γ takes 0 and 1, $\widehat{\mathbf{V}}_0 \triangleq [1]$ and $\widehat{\mathbf{V}}_1 = \widehat{\mathbf{V}}$, respectively.

$$L_y\left(P_o(\widehat{\mathbf{V}})\right) \triangleq \sum_{\mathbf{\Gamma}_j\in\mathbf{P}} c_j \cdot y_j\,, \; where\; y_j \in \mathbb{R}; \;\; L_y(1) = 1 \tag{8}$$

$$L_y\left(\begin{bmatrix} P_o^{1,1} \cdots p_o^{1,J} \\ \vdots \ddots \vdots \\ p_o^{J,1} \cdots p_o^{J,J} \end{bmatrix}\right) \triangleq \begin{bmatrix} L_y\left(P_o^{1,1}\right) \cdots L_y\left(P_o^{1,J}\right) \\ \vdots \quad \ddots \quad \vdots \\ L_y\left(P_o^{J,1}\right) \cdots L_y\left(P_o^{J,J}\right) \end{bmatrix}, \;\; J \in \mathbb{N} \tag{9}$$

$$\widehat{\mathbf{V}}_{\gamma} \triangleq \left[1\; V_0^{re,a} \ldots V_{N-1}^{im,c}\; \left(V_{N-1}^{re,a}\right)^2\; \left(V_0^{re,a} \cdot V_0^{re,b}\right) \ldots \left(V_{N-1}^{im,c}\right)^2 \; \left(V_0^{re,a}\right)^3 \;\; \left(\left(V_0^{re,a}\right)^2 \cdot V_0^{re,b}\right) \;\; \ldots \;\; \left(V_{N-1}^{re,c}\right)^{\gamma}\right], \;\; \forall \gamma \in \mathbb{N} \tag{10}$$

Based on definitions of Riesz linear function and $\widehat{\mathbf{V}}_{\gamma}$ in (8)-(10), the moment and localizing matrices are defined in (11)-(12a). ς takes the value by dividing the maximum monomial order of $P_o(\widehat{\mathbf{V}})$ by 2 and rounding up as shown in (12b).

$$\mathbf{M}_{\gamma} \triangleq L_y\left(\widehat{\mathbf{V}}_{\gamma} \cdot \widehat{\mathbf{V}}_{\gamma}^{\,T}\right) \tag{11}$$

$$\mathbf{M}_{\gamma-\varsigma}\left(P_o(\widehat{\mathbf{V}})\right) \triangleq L_y\left(P_o(\widehat{\mathbf{V}}) \cdot \widehat{\mathbf{V}}_{\gamma-\varsigma} \cdot \widehat{\mathbf{V}}_{\gamma-\varsigma}^{\,T}\right) \tag{12a}$$

$$\varsigma \triangleq \left\lceil \frac{1}{2} max_{\mathbf{\Gamma}_j\in\mathbf{P}} \left(\sum_{\eta_n^{re,\phi}\in\mathbf{\Gamma}_j} \eta_n^{re,\phi} + \sum_{\eta_n^{im,\phi}\in\mathbf{\Gamma}_j} \eta_n^{im,\phi}\right)\right\rceil \tag{12b}$$

The γ^{th}-order moment relaxation based SDP of the original ACOPF (7) is written as (13). The objective (13a) is presented in an epigraph form, where β_n^{ϕ} and ϑ_n^{ϕ} are defined in (13b)-(13c) as Schur's components. (13d)-(13g) correspond to (7b)-(7i), which are real and reactive power balance in each phase

$$min_{\mathbf{M}_\gamma,\beta_n^\phi,\vartheta_n^\phi} \sum_{n\in\mathbf{\Omega}_g}\sum_{\phi\in\mathbf{\Psi}}\beta_n^\phi - \sum_{n\in\mathbf{\Omega}_f}\sum_{\phi\in\mathbf{\Psi}}\vartheta_n^\phi \tag{13a}$$

$$\begin{bmatrix} \beta_n^\phi - c_{n,1}^\phi \cdot L_y\left(tr\left(\widehat{\mathbf{\Phi}}_{P,n}^\phi\cdot\widehat{\mathbf{V}}\cdot\widehat{\mathbf{V}}^T\right)+P_n^{\phi\,fix}\right) - c_{n,0}^\phi & -\sqrt{c_{n,2}^\phi}\cdot L_y\left(tr\left(\widehat{\mathbf{\Phi}}_{P,n}^\phi\cdot\widehat{\mathbf{V}}\cdot\widehat{\mathbf{V}}^T\right)+P_n^{\phi\,fix}\right) \\ -\sqrt{c_{n,2}^\phi}\cdot L_y\left(tr\left(\widehat{\mathbf{\Phi}}_{P,n}^\phi\cdot\widehat{\mathbf{V}}\cdot\widehat{\mathbf{V}}^T\right)+P_n^{\phi\,fix}\right) & 1 \end{bmatrix} \succcurlyeq 0, \quad \forall n\in\mathbf{\Omega}_g \tag{13b}$$

$$\begin{bmatrix} b_{n,1}^\phi\cdot L_y\left(-tr\left(\widehat{\mathbf{\Phi}}_{P,n}^\phi\cdot\widehat{\mathbf{V}}\cdot\widehat{\mathbf{V}}^T\right)\right)+b_{n,0}^\phi-\vartheta_n^\phi & \sqrt{-b_{n,2}^\phi}\cdot L_y\left(-tr\left(\widehat{\mathbf{\Phi}}_{P,n}^\phi\cdot\widehat{\mathbf{V}}\cdot\widehat{\mathbf{V}}^T\right)\right) \\ \sqrt{-b_{n,2}^\phi}\cdot L_y\left(-tr\left(\widehat{\mathbf{\Phi}}_{P,n}^\phi\cdot\widehat{\mathbf{V}}\cdot\widehat{\mathbf{V}}^T\right)\right) & 1 \end{bmatrix} \succcurlyeq 0, \quad \forall n\in\mathbf{\Omega}_f \tag{13c}$$

$$\mathbf{M}_{\gamma-1}\left(tr\left(\widehat{\mathbf{\Phi}}_{P,n}^\phi\cdot\widehat{\mathbf{V}}\cdot\widehat{\mathbf{V}}^T\right)-P_{Gn}^{\phi\,min}+P_n^{\phi\,fix}\right)\succcurlyeq 0;\quad \mathbf{M}_{\gamma-1}\left(-tr\left(\widehat{\mathbf{\Phi}}_{P,n}^\phi\cdot\widehat{\mathbf{V}}\cdot\widehat{\mathbf{V}}^T\right)+P_{Gn}^{\phi\,max}-P_n^{\phi\,fix}\right)\succcurlyeq 0,\quad \forall n\notin\mathbf{\Omega}_f \tag{13d}$$

$$\mathbf{M}_{\gamma-1}\left(tr\left(\widehat{\mathbf{\Phi}}_{Q,n}^\phi\cdot\widehat{\mathbf{V}}\cdot\widehat{\mathbf{V}}^T\right)-Q_{Gn}^{\phi\,min}+Q_n^{\phi\,fix}\right)\succcurlyeq 0;\quad \mathbf{M}_{\gamma-1}\left(-tr\left(\widehat{\mathbf{\Phi}}_{Q,n}^\phi\cdot\widehat{\mathbf{V}}\cdot\widehat{\mathbf{V}}^T\right)+Q_{Gn}^{\phi\,max}-Q_n^{\phi\,fix}\right)\succcurlyeq 0,\quad \forall n\notin\mathbf{\Omega}_f \tag{13e}$$

$$\mathbf{M}_{\gamma-1}\left(-tr\left(\widehat{\mathbf{\Phi}}_{P,n}^\phi\cdot\widehat{\mathbf{V}}\cdot\widehat{\mathbf{V}}^T\right)-P_{Dn}^{\phi\,min}\right)\succcurlyeq 0;\quad \mathbf{M}_{\gamma-1}\left(tr\left(\widehat{\mathbf{\Phi}}_{P,n}^\phi\cdot\widehat{\mathbf{V}}\cdot\widehat{\mathbf{V}}^T\right)+P_{Dn}^{\phi\,max}\right)\succcurlyeq 0,\quad \forall n\in\mathbf{\Omega}_f \tag{13f}$$

$$\mathbf{M}_{\gamma-1}\left(-tr\left(\widehat{\mathbf{\Phi}}_{Q,n}^\phi\cdot\widehat{\mathbf{V}}\cdot\widehat{\mathbf{V}}^T\right)-Q_{Dn}^{\phi\,min}\right)\succcurlyeq 0;\quad \mathbf{M}_{\gamma-1}\left(tr\left(\widehat{\mathbf{\Phi}}_{Q,n}^\phi\cdot\widehat{\mathbf{V}}\cdot\widehat{\mathbf{V}}^T\right)+Q_{Dn}^{\phi\,max}\right)\succcurlyeq 0,\quad \forall n\in\mathbf{\Omega}_f \tag{13g}$$

$$\mathbf{M}_{\gamma-1}\left(tr\left(\widehat{\mathbf{\Phi}}_{V,n}^\phi\cdot\widehat{\mathbf{V}}\cdot\widehat{\mathbf{V}}^T\right)-\left(\left|V_n^\phi\right|^{min}\right)^2\right)\succcurlyeq 0;\quad \mathbf{M}_{\gamma-1}\left(-tr\left(\widehat{\mathbf{\Phi}}_{V,n}^\phi\cdot\widehat{\mathbf{V}}\cdot\widehat{\mathbf{V}}^T\right)+\left(\left|V_n^\phi\right|^{max}\right)^2\right)\succcurlyeq 0,\quad \forall n\in\{\mathbf{\Omega}-0\} \tag{13h}$$

$$\mathbf{M}_\gamma \succcurlyeq 0 \tag{13i}$$

$$L_y\left(\left[V_0^{re,a}\ V_0^{re,b}\ V_0^{re,c}\ V_0^{im,a}\ V_0^{im,b}\ V_0^{im,c}\right]_\gamma^T\cdot\left[V_0^{re,a}\ V_0^{re,b}\ V_0^{re,c}\ V_0^{im,a}\ V_0^{im,b}\ V_0^{im,c}\right]_\gamma\right)=L_y\left(\widetilde{\mathbf{V}}_{0\gamma}\cdot\widetilde{\mathbf{V}}_{0\gamma}^T\right) \tag{13j}$$

of each bus. (13h) corresponds to (7j), which represents voltage limit in each phase of each bus. Since orders of (7b)-(7e) and (7j) are all 2 when written in polynomial forms, ς in (13d)-(13h) are all equal to 1. (13j) corresponds to (7h), which represents that substation bus voltages and their monomials defined in (10) are all fixed as pre-specified values

C. Exploiting Sparsity of the Distribution System Network

Computational burden of the moment relaxation based SDP model is highly dependent on the dimension of $\mathbf{M}_\gamma$ $\left(\begin{smallmatrix}\gamma\\ card(\mathbf{V})+\gamma\end{smallmatrix}\right)$, which could be easily intractable when γ is larger than two [19]. This section explores the sparsity of distribution systems, in order to reduce dimensions of $\mathbf{M}_\gamma$ and $\mathbf{M}_{\gamma-\varsigma}$ and accelerate computational performance for practical distribution systems.

Since P_{Gn}^ϕ, Q_{Gn}^ϕ, P_{Dn}^ϕ, and Q_{Dn}^ϕ can be represented by $\widehat{\mathbf{V}}$, $\widehat{\mathbf{V}}$ can be regarded as the only decision variables. (7) is said to have the running intersection property, if $\mathbf{V}$ (sub-vector of $\widehat{\mathbf{V}}$) can be partitioned into *P* overlapped sub-vectors $\mathbf{U}_k$ for *k*=0,…,*P*-1, which satisfy:

1) $\|\mathbf{V}\|_\infty$ has an upper bound;
2) All variables in each constraint belong to one and only one sub-vector $\mathbf{U}_k$;
3) The objective function is polynomial, and for every monomial in the objective function, all involved variables belong to one and only one sub-vector $\mathbf{U}_k$;
4) $\forall k\in\{1,\cdots,P-1\}$, $\exists s<k$ such that $\left(\mathbf{U}_k\cap(\cup_{i<k}\mathbf{U}_i)\right)\subseteq\mathbf{U}_s$.

Indeed, if a problem presents the running intersection property, its moment and localizing matrices can be divided into multiple submatrices as in (14a)-(14b). This derives an equivalent sparse moment relaxation, which has the same property of solution exactness as the corresponding moment relaxed model [21]. In the γth order moment relaxation model, one variable matrix $\mathbf{M}_\gamma$ is defined and required to be positive semidefinite. On the other hand, a set of $\mathbf{M}_\gamma^k$ is defined in the sparse moment relaxation model and required to be positive semidefinite. Indeed, all $\mathbf{M}_\gamma^k$ are submatrices of $\mathbf{M}_\gamma$. Thus, when $\mathbf{M}_\gamma$ is positive semidefinite, all $\mathbf{M}_\gamma^k$ are guaranteed to be positive semidefinite, whereas the converse is not true. In turn, moment relaxation is generally tighter than sparse moment relaxation. However, when Conditions 1)-4) are hold, the sparse moment relaxation is as tight as the moment relaxation, and the two models are equivalent [21].

$$\mathbf{M}_\gamma^k \triangleq L_y\left(\left(\widehat{\mathbf{U}}_k\right)_\gamma\cdot\left(\widehat{\mathbf{U}}_k\right)_\gamma^T\right) \tag{14a}$$

$$\mathbf{M}_{\gamma-\varsigma}^k\left(P_o\left(\widehat{\mathbf{U}}_k\right)\right)\triangleq L_y\left(P_o\left(\widehat{\mathbf{U}}_k\right)\cdot\left(\widehat{\mathbf{U}}_k\right)_{\gamma-\varsigma}\cdot\left(\widehat{\mathbf{U}}_k\right)_{\gamma-\varsigma}^T\right) \tag{14b}$$

where $\widehat{\mathbf{U}}_k=[1\ \ \mathbf{U}_k{}^T]^T$.

Multiple partitions may exist which satisfy all above four conditions. The partition with the smallest value of $max\{size(\mathbf{M}_\gamma^0),\cdots,size(\mathbf{M}_\gamma^{P-1})\}$ is sought in this paper, in order to reduce computational burden to the maximum extent. Indeed, for a radial distribution system, the best way is to build one subset for each bus (which is called a hub bus). That is, all three-phase variables of the hub bus and its adjacent buses constitute a subset, and the number of subsets is equal to the number of buses (i.e., *N*). In turn, *P*=*N* and each $\mathbf{U}_k$ for *k*=0,…,*N*-1 includes a set of voltage variables (i.e. elements in $\mathbf{V}$) associated with hub bus *k* and its adjacent buses. The value of $max\{size(\mathbf{M}_\gamma^0),\cdots,size(\mathbf{M}_\gamma^{N-1})\}$ is determined by the relaxation order and the connection degree of hub buses.

III. THE INEXACTNESS CONUNDRUM

A hierarchical moment relaxation approach for polynomial programming problems was discussed in [17], which converges to the global optimal solution of the origin problem when the relaxation order goes to infinite. The same conclusion can be made for the sparse moment relaxation model. Indeed, in certain cases, the global convergence may be achieved with a finite relaxation order [21]. Both first-order and second-order moment relaxation models have been used to exactly solve ACOPF problems [19]-[20].

However, it has to be acknowledged that inexactness may exist especially for low order moment relaxations, which means that optimal solution to the moment relaxation problem may not be feasible to the original ACOPF. The moment relaxation is exact if (15) is met, where ς^{max} is the maximum value among all ς [21]. In addition, if (15) is met but $rank(\mathbf{M}_\gamma)$ is larger than one, a decomposition algorism is needed to retrieve the optimal solution of $\mathbf{V}$ from $\mathbf{M}_\gamma$ [21]. For the sparse moment relaxation model, all $\mathbf{M}_\gamma^k$ need to satisfy (15) in order to guarantee exactness. Specifically, for the first-order relaxation $\gamma = 1$, $\mathbf{M}_0(1)$ is degraded into a scaler and its rank is one, and in turn (15) can be equivalently represented as (16).

$$rank(\mathbf{M}_\gamma) = rank\left(\mathbf{M}_{\gamma-\varsigma^{max}}(1)\right) \tag{15}$$

$$rank(\mathbf{M}_1) = rank(\mathbf{M}_0(1)) = 1 \tag{16}$$

To deal with possible inexactness, a hierarchical approach is proposed to obtain the global optimal solution or recover a good enough feasible solution based on the inexact solution. The hierarchical approach includes two major steps.

Step 1 First-Order Solving: Solve the first-order sparse moment relaxation model of ACOPF. If (16) is met, the global optimal solution is obtained, otherwise go to *Step 2.1*.

Step 2 Iterative Recovering:

2.1 The solution to the first-order sparse moment relaxation model obtained in *Step 1* is denoted as $\widehat{\mathbf{W}}_k$ for k=0,…,N-1, which are solutions to variable matrices $\mathbf{M}_1^k$ for k=0,…,N-1. Solve (17) to derive solution to the approximated voltage vector $\widehat{\mathbf{U}}_k$. The solution is denoted as $\widetilde{\mathbf{U}}_k$. It is worth mentioning that (17) represents a set of optimization problems corresponding to each k, which can be solved sequentially. That is, as sub-vectors $\widehat{\mathbf{U}}_k$ overlap with each other, overlapped variables $\widehat{\mathrm{U}}_{\mathrm{k}}^{\mathrm{s}}$ in the kth optimization problem are set via solutions from previous optimization problems 0,…,k-1 (17b). Specifically, voltages of the distribution substation bus in the first subset (i.e., k=0) are set as $\widetilde{\mathbf{V}}_0$. $\widetilde{\mathbf{U}}_k$ can be effectively derived from (17) via optimality conditions [22], where $\|\cdot\|_F$ is the Frobenius norm. $\widehat{\mathbf{U}}_k^s$ / $\widetilde{\mathbf{U}}_k^s$ represents the sub-vector constructed by variables in $\widehat{\mathbf{U}}_k/\widetilde{\mathbf{U}}_k$ that overlap with the subset $\widehat{\mathbf{U}}_s/\widetilde{\mathbf{U}}_s$.

$$min_{\widehat{\mathbf{U}}_k} \left\|\widehat{\mathbf{W}}_k - \widehat{\mathbf{U}}_k \cdot \widehat{\mathbf{U}}_k{}^T\right\|_F \tag{17a}$$

$$\widehat{\mathbf{U}}_k^s = \widetilde{\mathbf{U}}_s^k,\, 0 < k \le N-1,\ \forall s < k \tag{17b}$$

$$\left[V_0^{re,a}\ V_0^{re,b}\ V_0^{re,c}\ V_0^{im,a}\ V_0^{im,b}\ V_0^{im,c}\right]^T = \widetilde{\mathbf{V}}_0 \tag{17c}$$

2.2 Initialize $\mathbf{V}$ via $\widetilde{\mathbf{U}}_k$ obtained from *Step 2.1*. The initialized $\mathbf{V}$ is denoted as $\widetilde{\mathbf{V}}(0)$. Set iteration index $r = 0$.

2.3 Decouple the three-phase problem into three single-phase problems, by introducing pseudo fixed current injections in each single-phase problem to approximate the impact of the other two phases. Power injection to phase ϕ of bus n from all connected distribution lines can be represented in the complex form as shown on the left-hand-side of (18a), and further rewritten into two parts as shown on the right-hand-side of (18a). It can be seen that the first term on the right-hand-side of (18a) is only related to voltage variables in phase ϕ, and the second term is coupled with voltage variables of the other two phases. Pseudo injection current $I_{cp,n}^\phi$ is calculated as in (18b), which can be derived with known voltage values of the other two phases obtained from the previous iteration.

$$\widehat{\mathbf{V}}^T \cdot \left(\widehat{\mathbf{\Phi}}_{P,n}^\phi + j\cdot\widehat{\mathbf{\Phi}}_{Q,n}^\phi\right)\cdot\widehat{\mathbf{V}} = V_n^\phi \cdot \left(Y_{n,n}^{\phi,\phi}\cdot V_n^\phi + \sum_{m\in\mathbf{\Omega}_n} Y_{n,m}^{\phi,\phi}\cdot V_m^\phi\right)^H + V_n^\phi\cdot\left(\sum_{\rho\in\mathbf{\Psi}-\phi} Y_{n,n}^{\phi,\rho}\cdot V_n^\rho + \sum_{m\in\mathbf{\Omega}_n}\sum_{\rho\in\mathbf{\Psi}-\phi} Y_{n,m}^{\phi,\rho}\cdot V_m^\rho\right)^H \tag{18a}$$

$$I_{cp,n}^\phi = \left(\sum_{\rho\in\mathbf{\Psi}-\phi} Y_{n,n}^{\phi,\rho}\cdot V_n^\rho + \sum_{m\in\mathbf{\Omega}_n}\sum_{\rho\in\mathbf{\Psi}-\phi} Y_{n,m}^{\phi,\rho}\cdot V_m^\rho\right)^H\Big|_{\widetilde{\mathbf{V}}(r)} \tag{18b}$$

2.4 Solve three single-phase ACOPF problems with the first-order sparse moment relaxation based model. If solution for a certain single-phase problem does not satisfy (16), i.e., is inexact, the second-order sparse moment relaxation based model for this phase is further solved. If (15) is still not satisfied, go to *Step 2.5*; Otherwise, the voltage vector solution $\widetilde{\mathbf{V}}(r+1)$ is checked to see if (19) is satisfied: (i) If yes, a good enough feasible solution is obtained and the algorithm terminates; (ii) If not, update the voltage vector $\widetilde{\mathbf{V}}(r) = \widetilde{\mathbf{V}}(r+1)$ and $r = r+1$, and go to *Step 2.3*.

$$\left\|\widetilde{\mathbf{V}}(r+1) - \widetilde{\mathbf{V}}(r)\right\|_2 \le \varepsilon \tag{19}$$

2.5 For single-phase ACOPF problems whose second-order sparse moment relaxation is inexact, allow load over-satisfaction and resolve the first-order sparse moment relaxation. The solution is always exact [11]-[12]. The voltage vector solution $\widetilde{\mathbf{V}}(r+1)$ is checked to see if (19) is satisfied. If yes, the algorithm terminates; Otherwise, update the voltage vector $\widetilde{\mathbf{V}}(r) = \widetilde{\mathbf{V}}(r+1)$ and $r = r+1$, and go to *step 2.3*.

Proposition 1*:* In the proposed hierarchical recovering procedure, objective value of the original three-phase ACOPF problem with respect to optimal solutions of the three single-phase problems will converge.

Proposition 1 justifies the convergence property of the proposed hierarchical recovering method. The proof of Proposition 1 is included in the Appendix.

It is noted that the global optimal solution is obtained if the hierarchical approach terminates at *Step 1*. Otherwise, a good enough feasible solution to the original ACOPF can be recovered if the hierarchical approach terminates at *Step 2.4*. Quality of feasible solutions recovered from the iterative process can be justified via two facts: (i) the gap between the recovered feasible solution and the lower bound obtained in the first-order sparse moment relaxation model is very small; and (ii) $\mathbf{W}_k$ usually has only one large eigenvalue and all others are relatively small. This indicates that a rank-one feasible solution to the original ACOPF problem would be very close to current inexact solution $\mathbf{W}_k$ [22], and can be recovered via the iterative recovering process while using the current inexact solution as an initial point. Furthermore, if the hierarchical approach terminates at *Step 2.5*, the recovered solution may not be feasible to the origin ACOPF since load over-satisfaction is triggered. However, as over-satisfaction requires more power supply and in turn derives higher objective values, it is rarely observed that the iterative procedure terminates at *Step 2.5*. Indeed, as a distribution system could remain unchanged over a long time period, system operators can thoroughly examine parameter settings offline to further avoid such an inexact solution situation in real time operations. In addition, load over-satisfaction has also been discussed in the optimal Volt/VAR control problem [23] and the optimal power flow problem [24].

IV. Three-Phase Distribution LMPs

If the hierarchical approach terminates with the global optimal solution, duality gap between (13) and its Lagrangian dual is zero [25]. Sparse moment relaxation model holds the same property. Thus, at the global optimal solution, Lagrangian multipliers can accurately represent sensitivity of the objective function with respect to constraint bounds, which can be utilized to construct DLMPs of each phase in each bus of the distribution system. On the other hand, although a good enough feasible solution recovered from the hierarchical approach may not be global optimal to the origin unbalanced three-phase ACOPF problem, it is global optimal with zero duality gap for individual single-phase ACOPF problems. Thus, Lagrangian multipliers can still be useful for approximating DLMPs of each phase in each bus. However, it is emphasized that calculating approximate DLMPs for single-phase problems is a compromised approach, which is adopted only when the first-order sparse moment relaxation model of the three-phase problem cannot be solved exactly.

DLMP is derived based on (13). For the sake of discussion, $tr\left(\widehat{\mathbf{\Phi}}_{P,n}^{\phi} \cdot \widehat{\mathbf{V}} \cdot \widehat{\mathbf{V}}^{T}\right)$ is denoted as $\mathbf{\Lambda}$. Considering an incremental change of fixed load ΔP_{Dn}^{ϕ} at phase ϕ of bus n, the corresponding Lagrangian function of (13) is expressed in (20), where $\mathbf{L}_{s}(n)$ is defined in (21), and $\hat{\mathbf{L}}$ denotes terms that are not related to ΔP_{Dn}^{ϕ}. In (20), $\underline{\boldsymbol{Z}}_{n,\phi}^{P,G}$ and $\overline{\boldsymbol{Z}}_{n,\phi}^{P,G}$, $\underline{\boldsymbol{Z}}_{n,\phi}^{Q,G}$ and $\overline{\boldsymbol{Z}}_{n,\phi}^{Q,G}$, $\underline{\boldsymbol{Z}}_{n,\phi}^{P,D}$ and $\overline{\boldsymbol{Z}}_{n,\phi}^{P,D}$, $\underline{\boldsymbol{Z}}_{n,\phi}^{Q,D}$ and $\overline{\boldsymbol{Z}}_{n,\phi}^{Q,D}$, as well as $\underline{\boldsymbol{Z}}_{n,\phi}^{V}$ and $\overline{\boldsymbol{Z}}_{n,\phi}^{V}$ are Lagrangian multiplier matrices corresponding to (13d)-(13h), respectively. Furthermore, Lagrangian multiplier matrices corresponding to (13b)-(13c) are defined in (22).

$$\begin{bmatrix} 1 & \chi_{n,1}^{\phi} \\ \chi_{n,1}^{\phi} & \chi_{n,2}^{\phi} \end{bmatrix} \succcurlyeq 0,\ \forall n \in \mathbf{\Omega}_{g};\ \begin{bmatrix} -1 & \delta_{n,1}^{\phi} \\ \delta_{n,1}^{\phi} & \delta_{n,2}^{\phi} \end{bmatrix} \succcurlyeq 0,\ \forall n \in \mathbf{\Omega}_{f} \quad (22)$$

DLMP in phase ϕ of bus n can be calculated via (23). Solution to (13) is denoted as $\widetilde{\mathbf{M}}_{\gamma}$, and $\widetilde{\mathbf{M}}_{\gamma-1}$ represents submatrix in $\widetilde{\mathbf{M}}_{\gamma}$ that corresponds to $\mathbf{M}_{\gamma-1}(1)$ in $\mathbf{M}_{\gamma}$. It is worth mentioning that when $\gamma = 1$, $\widetilde{\mathbf{M}}_{\gamma-1}$ is 1 and all Lagrangian multiplier matrices are degraded to scalars. φ_{n}^{ϕ} is defined as in (24), which can be regarded as locational marginal price of reactive power.

Revenue is defined as the total money collected from loads minus the total money paid to DERs and the main grid. Money collected from a load is equal to the load value multiplying corresponding DLMP, and money paid to a DER is equal to its power generation multiplying corresponding DLMP. Total revenue of the distribution system can be calculated via (25), which includes revenues collected from fixed and flexible loads minus costs of electricity purchased from the distribution substation bus and DERs. In (25), $\widetilde{\mathbf{W}} = \left[1, \widetilde{\mathbf{V}}^{T}\right]^{T} \cdot \left[1, \widetilde{\mathbf{V}}^{T}\right]$, where $\widetilde{\mathbf{V}}$ is solution to $\mathbf{V}$.

$$\varphi_{n}^{\phi} = \begin{cases} tr\left(\left(\underline{\boldsymbol{Z}}_{n,\phi}^{Q,G} - \overline{\boldsymbol{Z}}_{n,\phi}^{Q,G}\right) \cdot \widetilde{\mathbf{M}}_{\gamma-1}\right), & \forall n \notin \mathbf{\Omega}_{f} \\ tr\left(\left(-\underline{\boldsymbol{Z}}_{n,\phi}^{Q,D} + \overline{\boldsymbol{Z}}_{n,\phi}^{Q,D}\right) \cdot \widetilde{\mathbf{M}}_{\gamma-1}\right), & \forall n \in \mathbf{\Omega}_{f} \end{cases} \quad (24)$$

V. Case Study

The modified IEEE 34-bus distribution system shown in Fig. 1 is used to analyze DLMPs and illustrate validation of the proposed hierarchical procedure. Three DERs GA, GB, and GC are connected at buses 11, 16, and 28, respectively. Three FLs are connected at buses 15, 21, and 31, respectively. GA is a single phase DER connected at phase *a*, while GB, GC, and the three FLs are three-phase assets. Detailed data for DERs and FLs are shown in Tables I-II. Voltages at the distribution substation bus are set as 1.05∠0°p.u., 1.05∠-120°p.u., and 1.05∠120°p.u. for phases *a*, *b*, and *c*, respectively. For all other buses, lower and upper phase voltage bounds are set as 0.95p.u. and 1.05p.u., respectively. As the rank of a matrix is equal to the number of its nonzero eigenvalues, the threshold of 5×10^{-4} is used to determine whether a numerical solution of an eigenvalue is nonzero. The moment relaxation based SDP model is solved by Mosek [26].

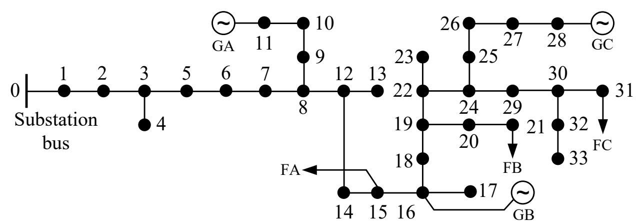

Fig. 1 The modified IEEE 34-bus distribution system

TABLE I Data of DERs

DER	Phase	$c_{g,2}$ ($\times10^{-5}$¢/kWh^2)	$c_{g,1}$ (¢/kWh)	$c_{g,0}$ (¢/h)	P_g^{max} (kW)	P_g^{min} (kW)	Q_g^{max} (kVar)	Q_g^{min} (kVar)
GA	*a*	225	7	100	450	0	850	0
	a	189	6.1	1000	1680	200	720	100
GB	*b*	203	6.3	1000	1680	200	780	100
	c	195	6.0	1000	1680	200	700	100
	a	110	5.1	400	1250	0	800	200
GC	*b*	133	5.2	400	1250	0	800	200
	c	133	5.6	400	1250	0	800	200

TABLE III Data of FLs

FL	Phase	$b_{d,2}$ ($\times10^{-5}$¢/kWh^2)	$b_{d,1}$ (¢/kWh)	$b_{d,0}$ (¢/h)	P_d^{max} (kW)	P_d^{min} (kW)	Q_d^{max} (kVar)	Q_d^{min} (kVar)
	a	-288	10.4	-200	230	0	120	100
FA	*b*	-578	12.2	-200	230	0	120	100
	c	-592	11.6	-200	230	0	120	100
	a	-255	16.0	-200	1500	0	750	350
FB	*b*	-298	16.7	-200	1500	0	750	350
	c	-243	15.7	-200	1500	0	750	350
	a	-452	12.9	-200	390	0	200	100
FC	*b*	-442	12.4	-200	460	0	220	100
	c	-436	12.3	-200	490	0	250	100

$$\mathbf{L}\left(\Delta P_{Dn}^{\phi}\right) = \hat{\mathbf{L}} + \mathbf{L}_s(n) + \begin{cases} tr\left(\underline{\mathbf{Z}}_{n,\phi}^{P,G} \cdot \mathbf{M}_{\gamma-1}\left(\mathbf{\Lambda} - P_{Gn}^{\phi\, min} + P_{n}^{\phi\, fix} + \Delta P_{Dn}^{\phi}\right)\right) + tr\left(\overline{\mathbf{Z}}_{n,\phi}^{P,G} \cdot \mathbf{M}_{\gamma-1}\left(-\mathbf{\Lambda} + P_{Gn}^{\phi\, max} - P_{n}^{\phi\, fix} - \Delta P_{Dn}^{\phi}\right)\right), & n \in \mathbf{\Omega}_g \\ tr\left(\underline{\mathbf{Z}}_{n,\phi}^{P,G} \cdot \mathbf{M}_{\gamma-1}\left(-\mathbf{\Lambda} - P_{Dn}^{\phi\, min} - \Delta P_{Dn}^{\phi}\right)\right) + tr\left(\overline{\mathbf{Z}}_{n,\phi}^{P,G} \cdot \mathbf{M}_{\gamma-1}\left(\mathbf{\Lambda} + P_{Dn}^{\phi\, max} + \Delta P_{Dn}^{\phi}\right)\right), & n \in \mathbf{\Omega}_f \\ tr\left(\underline{\mathbf{Z}}_{n,\phi}^{P,G} \cdot \mathbf{M}_{\gamma-1}\left(\mathbf{\Lambda} + P_{n}^{\phi\, fix} + \Delta P_{Dn}^{\phi}\right)\right) + tr\left(\overline{\mathbf{Z}}_{n,\phi}^{P,G} \cdot \mathbf{M}_{\gamma-1}\left(-\mathbf{\Lambda} - P_{n}^{\phi\, fix} - \Delta P_{Dn}^{\phi}\right)\right), & n \notin \mathbf{\Omega}_g + \mathbf{\Omega}_f \end{cases} \tag{20}$$

$$\mathbf{L}_s(n) = \begin{cases} c_{n,1}^{\phi}\left(L_y(\mathbf{\Lambda}) + P_n^{\phi\, fix} + \Delta P_{Dn}^{\phi}\right) + c_{n,0}^{\phi} + 2\chi_{n,1}^{\phi}\sqrt{c_{n,2}^{\phi}}\left(L_y(\mathbf{\Lambda}) + P_n^{\phi\, fix} + \Delta P_{Dn}^{\phi}\right) - \chi_{n,2}^{\phi}, & n \in \mathbf{\Omega}_g \\ -b_{n,1}^{\phi}\left(L_y(-\mathbf{\Lambda}) - \Delta P_{Dn}^{\phi}\right) - b_{n,0}^{\phi} + 2\delta_{n,1}^{\phi}\sqrt{-b_{n,2}^{\phi}}\left(L_y(-\mathbf{\Lambda}) - \Delta P_{Dn}^{\phi}\right) + \delta_{n,2}^{\phi}, & n \in \mathbf{\Omega}_f \\ 0, & n \notin \mathbf{\Omega}_g + \mathbf{\Omega}_f \end{cases} \tag{21}$$

$$DLMP_n^{\phi} = \frac{\partial L\left(\Delta P_{Dn}^{\phi}\right)}{\partial \Delta P_{Dn}^{\phi}} = \begin{cases} tr\left(\left(\underline{\mathbf{Z}}_{n,\phi}^{P,G} - \overline{\mathbf{Z}}_{n,\phi}^{P,G}\right) \cdot \widetilde{\mathbf{M}}_{\gamma-1}\right) + c_{n,1}^{\phi} + 2\chi_{n,1}^{\phi}\sqrt{c_{n,2}^{\phi}}, & n \in \mathbf{\Omega}_g \\ tr\left(\left(-\underline{\mathbf{Z}}_{n,\phi}^{P,D} + \overline{\mathbf{Z}}_{n,\phi}^{P,D}\right) \cdot \widetilde{\mathbf{M}}_{\gamma-1}\right) + b_{n,1}^{\phi} - 2\delta_{n,1}^{\phi}\sqrt{-b_{n,2}^{\phi}}, & n \in \mathbf{\Omega}_f \\ tr\left(\left(\underline{\mathbf{Z}}_{n,\phi}^{P,G} - \overline{\mathbf{Z}}_{n,\phi}^{P,G}\right) \cdot \widetilde{\mathbf{M}}_{\gamma-1}\right), & n \notin \mathbf{\Omega}_g + \mathbf{\Omega}_f \end{cases} \tag{23}$$

$$\begin{aligned} Rev = & \textstyle\sum_{n\in\mathbf{\Omega}-\mathbf{\Omega}_g-\mathbf{\Omega}_f} \sum_{\phi\in\mathbf{\Psi}} DLMP_n^{\phi} \cdot P_n^{\phi\, fix} + \sum_{n\in\mathbf{\Omega}_f} \sum_{\phi\in\mathbf{\Psi}} DLMP_n^{\phi} \cdot \left(-tr\left(\widehat{\mathbf{\Phi}}_{P,n}^{\phi} \cdot \widetilde{\mathbf{W}}\right)\right) - \sum_{\phi\in\mathbf{\Psi}} c_0^{\phi} \cdot tr\left(\widehat{\mathbf{\Phi}}_{P,0}^{\phi} \cdot \widetilde{\mathbf{W}}\right) \\ & - \textstyle\sum_{n\in\mathbf{\Omega}_g-0} \sum_{\phi\in\mathbf{\Psi}} DLMP_n^{\phi} \cdot \left(tr\left(\widehat{\mathbf{\Phi}}_{P,n}^{\phi} \cdot \widetilde{\mathbf{W}}\right) + P_n^{\phi\, fix}\right) \end{aligned} \tag{25}$$

A. DLMP

Electricity price of the distribution substation bus is set as 10¢/kWh. The unbalanced ACOPF is solved by the rank relaxed model, the first-order moment relaxation model, and the first-order sparse moment relaxation model, with computing times of 1064.5s, 1128.5s, and 1.59s, respectively. Solutions of both moment relaxation models are identical and both satisfy (16), which means that global optimal solution to the origin unbalanced ACOPF problem is obtained. The optimal operation cost is 1105.65$.

Three-phase DLMPs of all buses are shown in Fig. 2. Note that DLMPs of missing phases at certain buses are not presented. Fig. 2 shows that DLMPs of the three phases at the distribution substation bus 0 are all equal to 10¢/kWh, because the distribution substation bus acts as marginal units in all three phases. In addition, three-phase DLMPs at all other buses are relatively close, with the maximum difference of 1.07¢/kWh. The reason is that but voltage limits are not binding, and in turn differences in DLMPs are mainly caused by the increased system losses for supplying the load increment. The largest DLMP difference of two adjacent buses in the same phase is 0.19¢/kWh, which occurs at phase *c* of buses 22 and 24. The largest DLMP difference among three phases at the same bus is 0.30¢/kWh, which occurs between phases *a* and *c* at bus 31. Fig. 2 also shows that the ascending order of phase DLMPs is *c*, *b*, and *a* for most buses. The main reason is that phase *c* has the highest line impedance, and in turn introduces more losses than the other two phases.

It is also observed that $DLMP_n^{\phi}$ is much larger than φ_n^{ϕ}. The largest absolute value of φ_n^{ϕ} is 0.62¢/kVarh at phase *c* of bus 32, while $DLMP_n^{\phi}$ ranges from 10¢/kWh to 11.07¢/kWh. The reason is that the cost of reactive power is not explicitly included in the objective function (7a), and reactive power only indirectly impacts the objective function via its coupling with real power through bus voltages.

Fig. 2 shows that DLMPs are also impacted by the location of DERs. For instance, for buses 25-28 on a same feeder, if no DER is connected at bus 28, DLMPs of upstream buses (i.e., bus 25) should be smaller than those of downstream buses (i.e., bus 28). However, power injection from GC at bus 28 reverses power flow directions of lines 27-28 and 26-27 as compared to the case without GC. Indeed, loads at bus 26 are simultaneously supplied by electricity from GC and the upstream bus 25. Considering power flow directions of lines 27-28 and 26-27, from the DG point of view, more losses will be incurred by supplying the next load increment at bus 26 than buses 27 and 28. In turn, DLMPs at bus 26 are higher than those of its downstream and upstream buses in the same phase. However, this phenomenon is not observed on branches where GA and GB are connected to. Power output of GA is consumed by the large local fixed loads, and real power injection from GB does not reverse power flow directions on connected lines. In turn, the next load increment at downstream buses still causes more losses than upstream buses, and higher DLMPs are observed at downstream buses.

Bus voltage magnitude profiles of the three phases are shown in Fig. 3, which are all strictly within the lower and upper limits. That is, voltage constraints are not binding. It is observed that at most buses, voltage magnitude of phase *a* is the highest and the lowest occurs in phase *c*. This is mainly because line impedance of phase *c* is higher than those of the other two phases. It is also observed that a noticeable voltage magnitude drop occurs in phase *a* at buses 9-11. The reason is that lines connecting bus 8 to bus 11 are single-phase lines with phase *a* only, and a heavy load is connected at phase *a* of bus 11 which induces a significant voltage drop at bus 11.

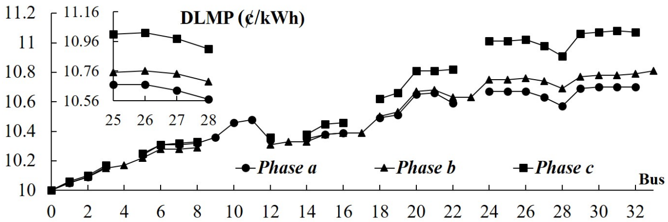

Fig. 2 Three-phase DLMPs of the modified IEEE 34-bus system

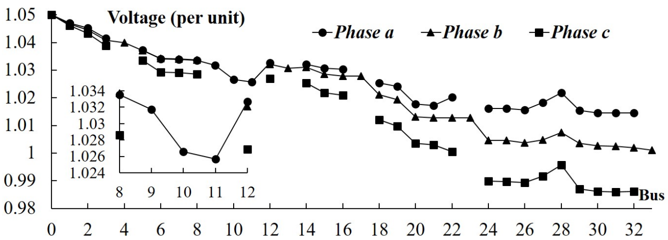

Fig. 3 Three-phase voltage magnitude profiles of the modified IEEE 34-bus system

Table II illustrates real power dispatches of FLs and DERs. It shows that the cheap unit GC is fully dispatched at its maximum capacity. On the other hand, since $b_{d,1}$ of FA in phase b is larger than those in phases a and c, 157.7kW is awarded in phase b comparing to 2.9kW and 97.3kW in phases a and c.

Reactive power dispatches of FLs and DERs are shown in Table III. Since reactive power production costs of DERs are not included in the objective function (7a), reactive power demands of FLs are binding at their lower limits and reactive power outputs of DERs are scheduled at their upper bounds. This would help enhance voltage magnitudes, reduce real power losses, and in turn decrease system costs.

TABLE II REAL POWER DISPATCHES OF FLS AND DERS (kW)

Phase	Distribution substation bus	FA	FB	FC	GA	GB	GC
a	3227.2	2.9	1047.1	242.9	450	897.5	1250
b	3395.4	157.7	1010.7	182.8	-	1055.9	1250
c	3325.4	97.3	1005.2	140.4	-	1067.6	1250

TABLE III REACTIVE POWER DISPATCHES OF FLS AND DERS (kVar)

Phase	Distribution substation bus	FA	FB	FC	GA	GB	GC
a	988.7	100	350	100	850	720	800
b	1653.9	100	350	100	-	780	800
c	1833.6	100	350	100	-	700	800

To further study the impact of DERs' location on DLMPs, GB is switched to buses 8 and 30. Fig. 4 presents DLMPs of phase c when GB is connected at buses 16, 8, and 30, respectively. It shows that DLMPs of all buses are decreased when GB is connected at bus 30, comparing with those when GB is at buses 16 and 8. As bus 30 is much closer to terminal of the feeder that suffers from low voltage magnitudes and to the load at bus 29, placing GB at bus 30 would help boost voltage at bus 30 and reduce power injection from upstream system. In turn, it would help reduce system losses and achieve lower DLMPs. Voltage magnitudes of bus 30 are 0.9833p.u., 0.9788p.u., and 0.9978p.u., when GB is connected at buses 16, 8, and 30, respectively. This shows the DER's effect on boosting voltages at connecting buses. In addition, the subgraph in Fig. 4 clearly shows that when GB is connected at bus 30, DLMP at bus 29 is higher than that of bus 30, which is caused by the reversed power flow on branch 29-30. The results indicate that locations of DERs are critical to system economical operation and also have significant impact on DLMPs.

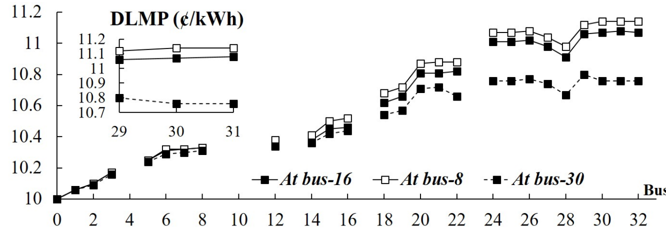

Fig. 4 DLMPs of phase c when GB is connected at three different buses

Revenue of the modified IEEE 34-bus distribution system is 2964¢, which is calculated via (25) with respect to DLMPs in Fig. 2 and real power dispatches in Table II. Table IV further shows revenues when all fixed loads are adjusted from 90% up to 120% of the original values. As shown in Table IV, with the increase in load, the total money collected from loads as well as the total payment to DERs and the main grid will also increase. However, the revenue may not be monotonically increasing. This is a main feature of LMPs for distribution power systems as discussed in [27]. Nevertheless, although the revenue is not strictly monotonous with the increase in loads, the revenue adequacy is achieved in all the cases.

TABLE IV THE SYSTEM REVENUE UNDER DIFFERENT LOAD LEVELS ($)

Load Level	90%	100%	110%	115%	120%
Payment from Loads	1647.57	1788.81	1925.20	2006.19	2078.93
Payment to Substation Bus and DERs	1624.01	1759.17	1896.22	1965.45	2034.97
Revenue	23.56	29.64	28.98	40.74	43.96

B. The Hierarchical Approach

The modified IEEE 34-bus system is revised to further illustrate the validation of the proposed hierarchical solution procedure. That is, all FLs are excluded, real power upper bounds of DERs are increased to 300% of original values, and reactive power upper bounds of DERs are decreased to 75%. In addition, $c_{g,1}$ of all DERs are set as zeros.

The ACOPF problem is solved by the first-order sparse moment relaxation model in 1.31s. The optimal system operation cost is 678.91$. Solutions to 27 out of 34 sub-matrices are not rank one. In all sub-matrices, $\widetilde{\mathbf{W}}_{31}$, namely the sub-matrix corresponding to the hub bus 31, has the most significant second largest nonzero eigenvalue of 0.0021.

It clearly shows that the first-order sparse moment relaxation model is inexact in this case. Based on the proposed hierarchy approach, $\widetilde{\mathbf{U}}_k$ is obtained by solving (17). The *Iterative Recovering* procedure is used to recover a feasible solution to the original ACOPF. Voltage $\widetilde{\mathbf{V}}_r$ converges after 9 iterations in 11.10s with respect to the threshold ε of 5×10^{-4}. In the iterative procedure, all single-phase sub-problems are exactly solved and the hierarchical approach terminates at *Step 2.4* of *Iterative Recovering* described in Section III. Thus, the recovered solution is a feasible solution of the original problem. Indeed, it is a good enough feasible solution since the objective value of the recovered solution is 681.89$, which is very close to the lower bound of 678.91$ from the first-order sparse moment relaxation model.

C. Discussion on the Inexactly Solved System

Based on our experience in numerical case studies, the first-order sparse moment relaxation can solve a broad set of radial distribution systems to derive exact solutions. Radial distribution systems which cannot be exactly solved by the first-order moment relaxation are usually constructed intentionally by manipulating certain system parameters for algorithm testing purposes. Indeed, finding a system that cannot be exactly solved via the first-order sparse moment relaxation may not be easy. [28] discussed several approaches which may contribute to constructing a system that cannot be solved exactly. However, the general approach to construct such a system remains unknown, and characters which could intuitively indicate that a system cannot be exactly solved have not been sufficiently studied.

Nevertheless, a small 4-bus system shown in Fig. 5 is provided to illustrate some interesting observations. A three-phase DER is connected at bus 2. Three-phase voltages of the substation bus are set as 1.05p.u. with 120 degree difference among phases. Voltage upper and lower bounds are set as 1.05p.u. and 0.95p.u., respectively. Electricity price at the substation bus is 10¢/kWh. Detailed line and load data are given in Tables V-VII. Load power factors are fixed, and load levels are adjusted for 80% to 110% of nominal values in Table VI with the step of 1%. Results with different real power load levels are shown in Table VIII. It can be seen that solution inexactness occurs in several discontinuous load levels. In addition, for load levels larger than 110% (up to the value that the system can physically supply) or less than 80%, inexactness never occurs again. That is, inexactness may not follow certain load patterns. In addition, for all inexactness cases, feasible solutions can be recovered by the proposed iterative hierarchical approach.

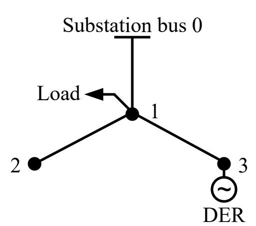

Fig. 5 A 4-bus example

TABLE V LINE PARAMETERS

Line	Length (feet)	Line admittance matrix in (ohms/ mile)
0-1	10000	$0.527-0.676j \quad -0.142+0.143j \quad -0.202+0.160j$
1-2	5000	$-0.142+0.143j \quad 0.465-0.669j \quad -0.130+0.131j$
1-3	5000	$-0.202+0.160j \quad -0.130+0.131 \quad 0.491-0.671j$

TABLE VI LOAD PARAMETERS

Bus	0			1			2			3		
	a	*b*	*c*	*a*	*b*	*c*	*a*	*b*	*c*	*a*	*b*	*c*
Real power (kW)	0	0	0	310	310	310	0	0	0	15	60	100
Reactive power (kVar)	0	0	0	175	175	175	0	0	0	90	30	60

TABLE VII DER PARAMETERS

Phase	$c_{n,2}^{\phi}$ (¢/kWh^2)	$c_{n,1}^{\phi}$ (¢/kWh)	$c_{n,0}^{\phi}$ (¢/h)	$P_{Gn}^{\phi\ max}$ (kW)	$P_{Gn}^{\phi\ min}$ (kW)	$Q_{Gn}^{\phi\ max}$ (kVar)	$Q_{Gn}^{\phi\ min}$ (kVar)
a	0.00214	0	0	350	0	150	0
b	0.00310	0	0	350	0	150	0
c	0.00233	0	0	350	0	150	0

TABLE VIII RESULTS OF THE 4-BUS SYSTEM

Load level	80%	81%	82%	83%	84%	85%	86%	87%
Is exact	Yes	Yes	Yes	Yes	Yes	No	No	Yes
Load level	88%	89%	90%	91%	92%	93%	94%	95%
Is exact	Yes	Yes	Yes	Yes	Yes	Yes	Yes	No
Load level	96%	97%	98%	99%	100%	101%	102%	103%
Is exact	No	No	No	No	No	No	No	No
Load level	104%	105%	106%	107%	108%	109%	110%	
Is exact	Yes	Yes	Yes	Yes	Yes	Yes	Yes	

VI. CONCLUSION

This paper discusses an effective DLMP calculation approach which can be used in restructuring process of the distribution sector. DLMPs of individual phases at each bus are derived by solving the unbalanced three-phase distribution ACOPF problem, with the objective of minimizing system operation cost. The ACOPF problem is formulated as a moment relaxation based SDP model, and the sparse moment relaxation technique is further adopted for improving computational performance. In addition, a hierarchical approach is proposed to deal with possible inexactness of the moment relaxation. Numerical results show that the proposed approach can effectively solve ACOPF problems of unbalanced three-phase distribution systems and provide effective DLMP signals. In addition, the impact of locations of DERs on DLMPs is analyzed. System revenue is also discussed to illustrate the performance of DLMPs as an effective price signal for restructuring the distribution sector.

APPENDIX

Proof of Proposition 1:

The three-phase ACOPF problem is represented as $min\ F_{\{\mathbf{V}_a,\mathbf{V}_b,\mathbf{V}_c\}\in\boldsymbol{\mathcal{F}}}(\mathbf{V}_a,\mathbf{V}_b,\mathbf{V}_c)$ for the sake of discussion, where $\mathbf{V}_a$, $\mathbf{V}_b$, and $\mathbf{V}_c$ are respectively voltage variables of phases *a*, *b*, and *c*, and $\boldsymbol{\mathcal{F}}$ represents feasible region of the three-phase ACOPF problem. Taking phase a for instance, the single-phase problem is written as $min\ F_{\{\mathbf{V}_a,\tilde{\mathbf{V}}_b,\tilde{\mathbf{V}}_c\}\in\boldsymbol{\mathcal{F}}}(\mathbf{V}_a,\tilde{\mathbf{V}}_b,\tilde{\mathbf{V}}_c)$, where superscript " ~ " means a given solution from a previous iteration. With the assumption that the single-phase problem can be solved to global optimal by first- or second-order sparse moment relaxation, the voltage vector of current iteration $\tilde{\mathbf{V}}_a$ can be recovered, which lies in the feasible region $\boldsymbol{\mathcal{F}}$. $F(\tilde{\mathbf{V}}_a,\tilde{\mathbf{V}}_b,\tilde{\mathbf{V}}_c)$ denotes the objective value of the original three-phase ACOPF problem with respect to given voltage solutions $\tilde{\mathbf{V}}_a$, $\tilde{\mathbf{V}}_b$, and $\tilde{\mathbf{V}}_c$.

Without loss of generality, in iteration r, phase a problem with given voltage values of the other two phases from the last iteration is solved as in (26a).

$$\tilde{\mathbf{V}}_a^r = arg\min_{\mathbf{V}_a^r} F(\mathbf{V}_a^r,\tilde{\mathbf{V}}_b^{r-1},\tilde{\mathbf{V}}_c^{r-1}) \tag{26a}$$

Similarly, phase *b* and phase *c* problems are solved via (26b) and (26c) successively.

$$\tilde{\mathbf{V}}_b^r = arg\min_{\mathbf{V}_b^r} F\left(\tilde{\mathbf{V}}_a^r, \mathbf{V}_b^r, \tilde{\mathbf{V}}_c^{r-1}\right) \tag{26b}$$

$$\tilde{\mathbf{V}}_c^r = arg\min_{\mathbf{V}_c^r} F\left(\tilde{\mathbf{V}}_a^r, \tilde{\mathbf{V}}_b^r, \mathbf{V}_c^r\right) \tag{26c}$$

From (26), (27) can be obtained.

$$F\left(\mathbf{V}_a^r, \tilde{\mathbf{V}}_b^{r-1}, \tilde{\mathbf{V}}_c^{r-1}\right) \geq F\left(\tilde{\mathbf{V}}_a^r, \tilde{\mathbf{V}}_b^{r-1}, \tilde{\mathbf{V}}_c^{r-1}\right) \tag{27a}$$

$$F\left(\tilde{\mathbf{V}}_a^r, \mathbf{V}_b^r, \tilde{\mathbf{V}}_c^{r-1}\right) \geq F\left(\tilde{\mathbf{V}}_a^r, \tilde{\mathbf{V}}_b^r, \tilde{\mathbf{V}}_c^{r-1}\right) \tag{27b}$$

$$F\left(\tilde{\mathbf{V}}_a^r, \tilde{\mathbf{V}}_b^r, \mathbf{V}_c^r\right) \geq F\left(\tilde{\mathbf{V}}_a^r, \tilde{\mathbf{V}}_b^r, \tilde{\mathbf{V}}_c^r\right) \tag{27c}$$

Considering the objective value $F\left(\tilde{\mathbf{V}}_a^{r-1}, \tilde{\mathbf{V}}_b^{r-1}, \tilde{\mathbf{V}}_c^{r-1}\right)$ of iteration $(\mathrm{r}-1)$, (28) can be derived.

$$F\left(\tilde{\mathbf{V}}_a^{r-1}, \tilde{\mathbf{V}}_b^{r-1}, \tilde{\mathbf{V}}_c^{r-1}\right) \geq min\, F\left(\mathbf{V}_a^r, \tilde{\mathbf{V}}_b^{r-1}, \tilde{\mathbf{V}}_c^{r-1}\right) = F\left(\tilde{\mathbf{V}}_a^r, \tilde{\mathbf{V}}_b^{r-1}, \tilde{\mathbf{V}}_c^{r-1}\right) \tag{28a}$$

$$F\left(\tilde{\mathbf{V}}_a^r, \tilde{\mathbf{V}}_b^{r-1}, \tilde{\mathbf{V}}_c^{r-1}\right) \geq min\, F\left(\tilde{\mathbf{V}}_a^r, \mathbf{V}_b^r, \tilde{\mathbf{V}}_c^{r-1}\right) = F\left(\tilde{\mathbf{V}}_a^r, \tilde{\mathbf{V}}_b^r, \tilde{\mathbf{V}}_c^{r-1}\right) \tag{28b}$$

$$F\left(\tilde{\mathbf{V}}_a^r, \tilde{\mathbf{V}}_b^r, \tilde{\mathbf{V}}_c^{r-1}\right) \geq min\, F\left(\tilde{\mathbf{V}}_a^r, \tilde{\mathbf{V}}_b^r, \mathbf{V}_c^r\right) = F\left(\tilde{\mathbf{V}}_a^r, \tilde{\mathbf{V}}_b^r, \tilde{\mathbf{V}}_c^r\right) \tag{28c}$$

From (28), (29) can be finally obtained.

$$F\left(\tilde{\mathbf{V}}_a^{r-1}, \tilde{\mathbf{V}}_b^{r-1}, \tilde{\mathbf{V}}_c^{r-1}\right) \geq F\left(\tilde{\mathbf{V}}_a^r, \tilde{\mathbf{V}}_b^r, \tilde{\mathbf{V}}_c^r\right) \tag{29}$$

(29) shows that along the proposed iterative procedure, objective value of the original three-phase ACOPF problem is monotonously decreasing. Since a lower bound to the original three-phase ACOPF problem can be calculated via the first-order sparse moment relaxation solution, the monotonously decreasing sequence $F\left(\tilde{\mathbf{V}}_a^r, \tilde{\mathbf{V}}_b^r, \tilde{\mathbf{V}}_c^r\right)$ from the proposed iterative procedure will finally converge to a certain value limited by this lower bound. ■

REFERENCES

[1] G.T. Heydt, "The next generation of power distribution systems," *IEEE Trans. Smart Grid.*, vol. 4, no. 3, pp. 1464–1475, Sep. 2013.

[2] K. Shaloudegi, N. Madinehi, S.H. Hosseinian, and H.A. Abyaneh, "A novel policy for locational marginal price calculation in distribution systems based on loss reduction allocation using game theory," *IEEE Trans. Power Syst.*, vol. 27, no. 2, pp. 811–820, May 2012.

[3] P.M. Sotkiewicz and J.M, Vignolo, "Nodal pricing for distribution networks: efficient pricing for efficiency enhancing DG," *IEEE Trans. Power Syst.*, vol. 21, no. 2, pp. 1013–1014, May. 2006.

[4] S. Huang, Q. Wu, S.S. Oren, R. Li, and Z. Liu, "Distribution locational marginal pricing though quadratic programming for congestion management in distribution networks," *IEEE Trans. Power Syst.*, vol. 30, no. 4, pp. 2170–2178, Jul. 2015.

[5] P.M. Sotkiewicz and J.M. Vignolo, "Nodal pricing for distributionnetworks: Efficient pricing for efficiency enhancing DG," IEEE *Trans. Power Syst.*, vol. 21, no. 2, pp. 1013–1014, May 2006.

[6] E.D. Anese, H. Zhu, and G.B. Giannakis, "Distributed optimal power flow for smart microgrids," *IEEE Trans. Power Smart Grid.*, vol. 4, no. 3, pp. 1464–1475, Sep. 2013.

[7] J. Lavaei and S.H. Low, "Zero duality gap in optimal power flow problem," *IEEE Trans. Power Syst.*, vol. 27, no. 1, pp. 92–106, Feb. 2012.

[8] D.K. Molzahn, S.S. Baghsorkhi, and I.A. Hiskens, "Semidefinite relaxations of equivalent optimal power flow problems: an illustration example," *IEEE International Symposium on Circuits and Systems (ISCAS)*, 2015.

[9] D.K. Molzahn, B.C. Lesieutre, and C.L. DeMarco, "Investigation of non-zero duality gap solution to a semidefinite relaxation of the optimal power flow problem," *47th Hawaii International Conference on System Sciences* (*HICSS*), 2014.

[10] B.C. Lesieutre, D.K. Molzahn, A.R. Bordenand, and C.L. Demarco, "Examining the limits of the application of semidefinite programming to power flow problems," *49th Annual Allerton Conference on Communication, Control, and Computing* (*Allerton*), 2011.

[11] S. Bose, D. Gayme, and S. Low, "Optimal power flow over tree networks," *49th Annual Allerton Conference on Communication, Control, and Computing* (*Allerton*), 2011.

[12] B. Zhang and D. Tse, "Geometry of injection regions of power networks," *IEEE Trans. Power Syst.*, vol. 28, no. 2, pp. 788–796, May 2013.

[13] J. Lavaei, D. Tse, and B. Zhang, "Geometry of power flows and optimization in distribution networks," *IEEE Trans. Power Syst.*, vol. 29, no. 2, pp. 572–583, Mar. 2014.

[14] S. Sojoudi and J. Lavaei, "Exactness of semidefinite relaxations for nonlinear optimization problems with underlying graph structure," *SIAM Journal on Optimization*, vol. 24, pp. 1746–1778, 2015.

[15] S. Low, "Convex relaxation of optimal power flow—part I: formulation and equivalence," *IEEE Trans. Control Network Syst.*, vol. 1, no. 1, pp. 15–27, Mar. 2014.

[16] S. Low, "Convex relaxation of optimal power flow, II: Exactness," *IEEE Trans. Control Network Syst.*, vol. 1, no. 2, pp. 177–189, Jun. 2014.

[17] J. Lasserre, "Global optimization problems with polynomials and the problem of moments," *SIAM Journal on Optimization*, vol. 11, no. 3, pp. 796–817, 2001.

[18] C. Josz, J. Maeght, and J. C. Gilbert, "Application of the moment-sos approach to global optimization of the OPF problem," *IEEE Trans. Power Syst.*, vol. 30, no. 1, pp. 463–469, Jan. 2015.

[19] D.K. Molzahn and I.A. Hiskens, "Sparsity-exploiting moment based relaxations of the optimal power flow problem," *IEEE Trans. Power Syst.*, vol. 30, no. 6, pp. 3168–3180, Nov. 2015.

[20] H. Waki, S. Kim, M. Kojima, and M. Muramatsu, "Sums of squares and semidefinite programming relaxations for polynomial optimization problems with structured sparsity," *SIAM Journal on Optimization*, vol. 17, no. 1, pp. 796–817, 2006.

[21] J. Lasserre, "An introduction to polynomial and semi-algebraic optimization," Cambridge University Press, United Kingdom, 2015.

[22] T. Erseghe and S. Tomasin, "Power flow optimization for smart microgrid by SDP relaxation on linear networks," *IEEE Trans. Power Smart Grid.*, vol. 4, no. 2, pp. 751–762, Jun. 2013.

[23] M. Farivar, C. R. Clarke, S. H. Low, and K.M. Chandy, "Inverter VAR control for distribution systems with renewables," in Proc. 2011 IEEE Int. Conf. Smart Grid Commun., pp. 457-462, 2011.

[24] S. Sojoudi, R. Madani, and J. Lavaei, "Low-rank solution of convex relaxation for optimal power flow problem," in *Proc*. 2013 IEEE Int. Conf. Smart Grid Commun., pp.636-641, 2013.

[25] C. Josz and D. Henrion, "Strong Duality in Lasserre's Hierarchy for Polynomial Optimization," *Springer, Optimiz. Letters*, 2015.

[26] Mosek, http://docs.mosek.com/7.0/toolbox/.

[27] J. Reneses, M.P.R. Ortega, "Distribution pricing: theoretical principles and practical approaches," *IET Gener. Transm. Distrib.*, vol. 8, no. 10, pp. 1645-1655, 2014.

[28] C. Chen, A. Atamturk, and S.S. Oren, "Bound tightening for the alternating current optimal power flow problem," *IEEE Trans. Power Syst.*, vol. 31, no. 5, pp. 3729-3736, Sep. 2016.

BIOGRAPHIES

Yikui Liu (S'15) received the B.S. degree in electrical engineering and automation from Nanjing Institute of Technology, China, in 2012 and the M.S. degree in power system and automation from Sichuan University, China, in 2015. He is currently pursuing the Ph.D. degree with Electrical and Computer Engineering Department, Clarkson University, USA. His current research interest is power market and OPF in distribution system.

Jie Li (M'14) received the B.S. degree in information engineering from Xi'an Jiaotong University in 2003 and the M.S. degree in system engineering from Xi'an Jiaotong University, China in 2006, and the Ph.D. degree from the Illinois Institute of Technology (IIT), Chicago, in 2012. From 2006 to 2008, she was a Research Engineer with IBM China Research Lab. From 2012 to 2013, she was a Power System Application Engineer with GE Energy Consulting. Presently, she is an Assistant Professor in the Electrical and Computer Engineering Department at Clarkson University. Her research interests include power systems restructuring and bidding strategy.

Lei Wu (SM'13) received the B.S. degree in electrical engineering and the M.S. degree in systems engineering from Xi'an Jiaotong University, Xi'an, China, in 2001 and 2004, respectively, and the Ph.D. degree in electrical engineering from Illinois Institute of Technology (IIT), Chicago, IL, USA, in 2008. From 2008 to 2010, he was a Senior Research Associate with the Robert W. Galvin Center for Electricity Innovation, IIT. He worked as summer Visiting Faculty at NYISO in 2012. Currently, he is an Associate Professor with the Electrical and Computer Engineering Department, Clarkson University, Potsdam, NY, USA. His research interests include power systems operation and planning, energy economics, and community resilience microgrid.